JOURNAL OF MATERIALS SCIENCE 21 (1986) 923–930

Effect of multiple strain–anneal cycles on the 1000° C creep behaviour of $\gamma/\gamma'-\alpha$

J. D. WHITTENBERGER, B. C. BUZEK
NASA–Lewis Research Center, Cleveland, Ohio 44135, USA
G. WIRTH
DFVLR, 90 Koeln 5000, West Germany

An investigation of the influence of multiple strain–anneal cycles on the 1000° C creep behaviour of the directionally solidified eutectic alloy $\gamma/\gamma'-\alpha$ has been undertaken. Cycles consisted of swageing at room temperature or 900° C by about 5 to 10% per pass followed by annealing at 900° C, and were repeated to total strains of approximately 10, 30 and 50%. Transmission electron microscopy (TEM) of strain–annealed materials revealed that three-dimensional dislocation networks were introduced into the γ' matrix, but very little work remained in the α fibres. Constant-velocity creep testing indicated that all thermomechanical processing schedules improved the creep strength for strain rates $\geqslant 2 \times 10^{-6}\,\text{sec}^{-1}$; however only strain–annealing with a total of 13% work at room temperature (RT13) improved the behaviour at strain rates $\sim 2 \times 10^{-7}\,\text{sec}^{-1}$. The advantage of RT13 processing over as-grown materials at lower strain rates was confirmed by constant-load creep testing. It was also shown that 900° C annealing slightly improves the 1000° C creep properties in comparison to as-grown alloys. TEM of crept materials indicated that the active creep mechanism had been changed from dislocation pile-ups at fibres in as-grown alloys to dislocations being stopped by sub-boundaries in the γ' matrix for RT13.

1. Introduction

Recently an attempt was made [1] to improve the 1000°C creep strength of the directionally solidified eutectic (DSE) alloy $\gamma/\gamma'-\alpha$ through thermomechanical processing (TMP). As-grown materials were swaged by approximately 10 and 25% in single passes at 750, 900 and 1050° C to introduce a dislocation substructure. Transmission electron microscopy (TEM) of the deformed materials revealed that a cold-work type of structure was imparted rather than the intended subgrains; furthermore constant, slow velocity compression testing indicated that none of the working conditions increased the creep strength. But it was noted that samples annealed for 1 h at 900° C possessed somewhat better properties than the as-grown alloy.

The following describes a further effort to improve the creep strength of $\gamma/\gamma'-\alpha$ through thermomechanical processing. Such a study is reasonable, since attempts to alloy for better properties [2, 3] have not been successful, and secondary working (forging, for example) would simplify fabrication of hardware from DSE bars. As-grown materials were subjected to multiple strain–anneal cycles where each step involved small amounts of work at 900° C or room temperature followed by annealing at 900° C. For baseline purposes and to investigate the effect of simple heat treatment, additionally $\gamma/\gamma'-\alpha$ was given the same annealing schedule as the worked alloys. TEM was used as the primary materialographic tool, and creep behaviour was evaluated by both constant-velocity and constant-load compression testing at 1000° C.

2. Experimental procedures

Approximately 8 mm diameter, 300 mm long $\gamma/\gamma'-\alpha$ bars of nominal composition Ni–32.3 Mo–6.3 Al (wt %) were grown at $17\,\text{mm}\,\text{h}^{-1}$ with a modified Bridgeman technique. Five bars without growth faults were selected, two ~ 120 mm lengths cut from the central portion of each bar, and these were encapsulated in 0.9 mm wall stainless steel tubing. Three bars were designated for 900° C TMP with one half of each being subjected to the strain–anneal cycles while the other portion received only the heat-treatment steps. Three halves from the remaining two bars were used for the strain–anneal cycles involving ambient temperature work, and the remaining half was retained for measurement of as-grown properties.

All working was accomplished by swageing. For the 900° C processing each cycle, except the first, consisted of a 3 h anneal, followed by swageing by approximately 10 %, and then air-cooling to room temperature. A 1 h heat treatment prior to swageing was utilized for the first cycle, and a 3 h anneal was given after the last swageing pass. The materials worked at room temperature were basically given the same schedule as the above, except that after swageing the specimens were annealed at 900° C and then air-cooled. To minimize the twisting of the α fibres in the direction of die rotation, the worked materials were turned end for end after each cycle.

0022–2461/86 $03.00 + .12

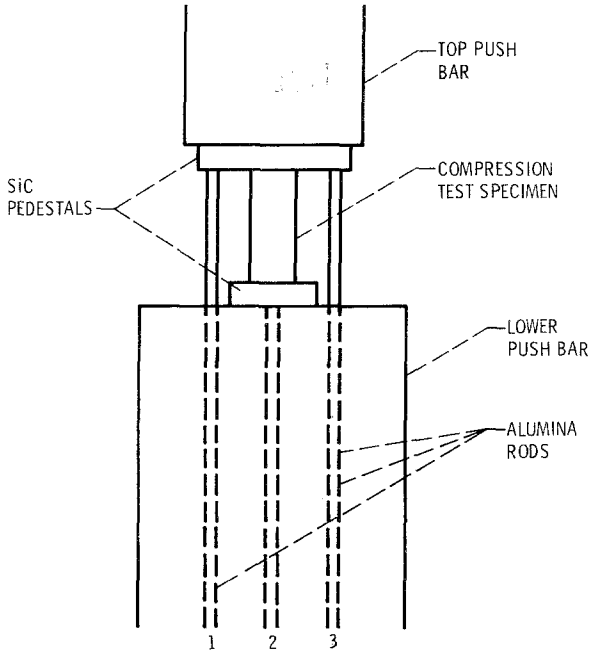

Figure 1 Geometry of compressive creep test. Alumina rods (1 and 3) attached to a linear variable differential transducer (LVDT) coil, and rod (2) attached to LVDT core.

Although it was desirable to introduce ~5% work in the $\gamma/\gamma'-\alpha$ per swageing pass, this was not always practical due to the availibility of dies and the unknown apportionment of strain between the stainless steel cladding and the $\gamma/\gamma'-\alpha$. Materials were worked at 900° C for 2, 4 and 7 cycles while alloys swaged at ambient temperature were subjected to 3, 5 and 7 cycles. These choices were made in an attempt to introduce nominally equal amounts of work at three levels. An additional room-temperature cycle at the lower levels was included, because it was felt that the very high strength of $\gamma/\gamma'-\alpha$ in comparison to the cladding would concentrate the majority of the strain in the stainless steel.

Right cylindrical specimens 5 mm in diameter and 10 mm in length were taken for all material conditions. These were compression-tested in air at 1000° C under constant-velocity conditions imposed by a universal test machine where the approximate strain rates ranged from 2×10^{-5} to 2×10^{-7} sec^{-1}. Autographically recorded load–time curves were converted to true stresses and strains by the offset method [4] and the assumption of constant volume.

In order to determine behaviour at slower strain rates, several constant-load, 1000° C compression creep tests were undertaken. In this case strain was determined from a continuous record of the relative motion of an upper SiC push bar in relationship to the bottom of the test sample (Fig. 1). Pieces of tungsten foil ~25 μm thick were inserted between the ends of the test specimens and the SiC pedestals to prevent welding. Temperatures were monitored through Type R thermocouples wired to the top and bottom of each test sample. During testing, the temperature was maintained to within 1° C of the set point, and the difference between the two thermocouples readings never exceeded 3° C. Specimens were slowly heated to temperature over 2+ h while a small stress (about 2 MPa) was applied by the upper push bar to maintain alignment. True stresses and strain rates were calculated from the standard definitions and the principle of volume conservation. The calculated strain at the end of each test agreed well (± 10 %) with that determined by the measured change in length; however, for consistency, calculated strains were normalized to the actual length change.

The microstructures of the materials prior to creep testing and of a few specimens after testing were evaluated by TEM. Approximately 400 μm thick sections were cut with a diamond saw, mechanically ground on 600 grit SiC paper to ~100 μm, and electrochemically prepared for observation with a one part sulphuric acid–5 parts ethanol mixture (parts by volume), cooled to 3° C in a Fishione Twin Jet polisher operating at 25 mA and 55 volts.

Additional details concerning the directional solidification process and the $\gamma/\gamma'-\alpha$ alloy can be found elsewhere [1, 5], as can further information on the constant-velocity test procedures [1, 6].

3. Results

3.1. Thermomechanically processed materials

Table I presents a summary of the TMP schedules, the total strain imparted into $\gamma/\gamma'-\alpha$ by swageing and the annealing time at 900° C for each condition. The overall work was calculated from the lengths of each piece before and after swageing. Estimates of the strain based on measured diameters of materialographically prepared cross-sections were also made and generally agreed with those from length changes; however, these estimates are subject to more error due to the non-uniform nature of the DSE bars, so they are not reported. Contrary to our original belief that swageing would be more difficult at room temperature, the strain data in Table I indicate that there is little difference between the swageability of $\gamma/\gamma'-\alpha$ at 900° C or ambient temperature.

Typical TEM photomicrographs of the thermomechanically processed materials are presented in Fig. 2. The structure of as-grown $\gamma/\gamma'-\alpha$ is shown in Fig. 2a, where the square-shaped molybdenum-rich fibres lies in a γ' matrix (light grey) throughout which are islands of γ (dark grey). Heat treatments for total times of 7, 13 and 22 h yielded similar microstructures

TABLE I Summary of strain–anneal schedules

Number of cycles	Temperature of swageing (° C)	True work* (%)	Total time at 900° C (h)
2	–	–	7
2	900	9	7†
4	–	–	13
4	900	30	13†
7	–	–	22
7	900	46	22†
3	25	13	9
5	25	35	15
7	25	56	34‡
As-grown		–	–

*Error estimated as ± 1%.
†1 h at 900° C prior to first pass.
‡Anneal after sixth pass inadvertently conducted for 16 h.

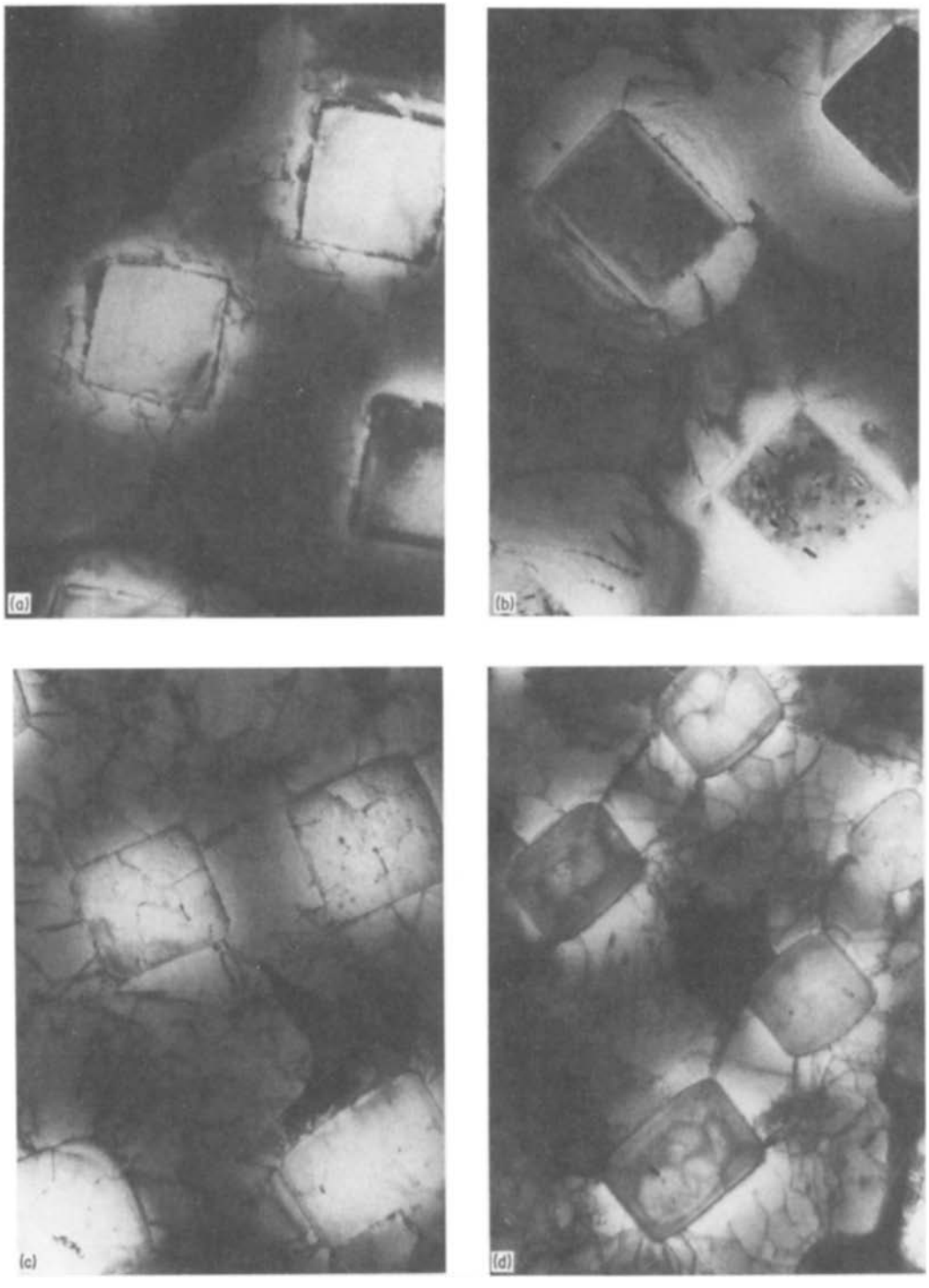

Figure 2 Typical microstructures in thermomechanically processed $\gamma/\gamma'-\alpha$. (a) As-grown, (b) annealed 7 h at 900° C, (c) two 900° C swageing cycles, (d) three room-temperature swageing cycles, (e) seven 900° C swageing cycles, (f) seven room-temperature swageing cycles.

(Fig. 2b) where some rounding or faceting of the corners of the α fibres and precipitation within the molybdenum phase occurred. Annealing also brought out the misfit dislocations between γ and γ', and the dislocation density within these phases seemed to decrease with increasing time at temperature.

Two strain-anneal cycles involving 900° C work and three cycles with room temperature swageing yielded similar structures (Figs. 2c and d). For these conditions, relatively loose three-dimensional dislocation networks were introduced into γ'. Behaviour inside γ could not be determined as this phase became totally opaque, probably due to the imparted work and fine γ' precipitation. Rounding/faceting of the fibre corners also occurred, and a few individual, isolated dislocations appeared within the molybdenum-rich phase. In addition the fibres seem to be more misshapen by ambient temperature swageing (Fig. 2d) than 900° C working (Fig. 2c).

TMP to higher strains yielded microstructures (Figs. 2e and f) which are similar to those for the lower work levels (Figs. 2c and d); however, the overall effects were generally intensified by the greater amounts of strain. In particular the fibres became more misshapen, and the dislocations density within γ' increased to the point where it was almost impossible

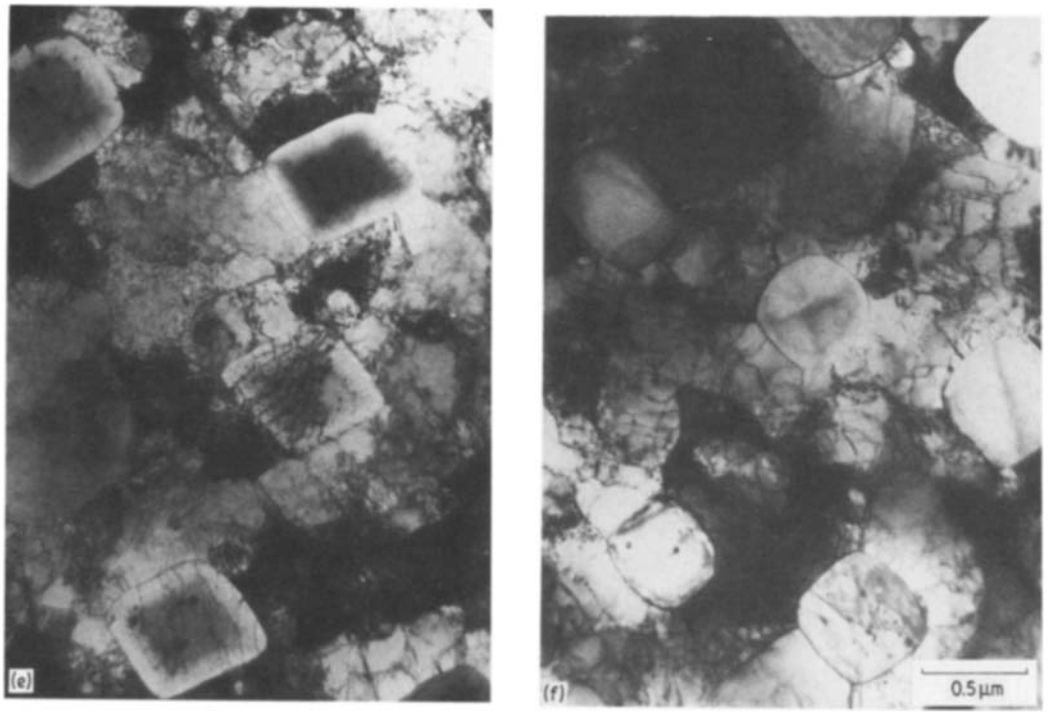

Figure 2 Continued.

to identify networks. The only obvious difference between the two working temperatures was that 900° C strain–annealing left dislocations, and in one instance a substructure, in the fibres (Fig. 2e), while room-temperature work followed by heat treatment produced a dislocation-free α phase (Fig. 2f).

3.2. Mechanical properties

Examples of stress–strain diagrams determined from constant-velocity compression testing are shown in Fig. 3 for two TMP conditions. The general behaviour exhibited by the materials consisted of work-hardening through ~0.5 to 2% strain, followed by further flow at an approximately constant or very slowly decreasing stress to a strain of 5 % or more. Materials swaged at 900° C deviated somewhat from this pattern at the fastest strain rate, where the constant-flow stress was only reached after 3 to 4% strain.

Data for flow stress, σ, and strain rate, $\dot{\varepsilon}$, were taken from each stress–strain diagram where σ, ε are average values from the approximately constant-stress regime. Because of the test method, the data are clumped together and cannot be adequately separated in the usual log–log graph; hence flow stress and approximate strain rates are tabulated (Table II). Comparison of these data for the various TMP condition reveals

1. The behaviour of as-grown and annealed $\gamma/\gamma'-\alpha$ is similar.
2. At strain rates $> 2 \times 10^{-6}\,\text{sec}^{-1}$ both room temperature and 900° C, swageing improved the 1000° C flow strength in comparison to either as-grown or annealed materials; however the improvement is independent of the amount of prior strain.
3. At strain rate $\sim 2 \times 10^{-7}\,\text{sec}^{-1}$ the flow stress for 900° C swaged materials decreases with increasing prior strain.
4. For materials swaged at ambient temperature and tested $\dot{\varepsilon} \sim 2 \times 10^{-7}\,\text{sec}^{-1}$, 30% or more work had essentially no effect on the flow strength in comparison to as-grown or annealed $\gamma/\gamma'-\alpha$, while the material worked by 13% in three cycles (hereby designated as RT13) has a flow stress about 15% greater than that measured for as-grown or annealed materials.

To see if the positive effect of the RT13 condition could be maintained at creep rates of commercial interest ($\sim 10^{-8}\,\text{sec}^{-1}$), constant-load creep tests were

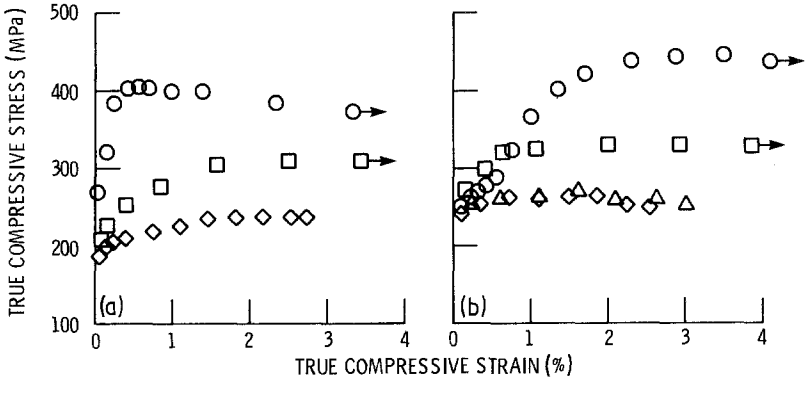

Figure 3 True compressive stress–strain diagrams for thermomechanically processed $\gamma/\gamma'-\alpha$. (a) Annealed 7 h at 900° C, (b) three strain–anneal cycles with room-temperature swageing. Approximate strain rate (sec^{-1}): (○) 2.15×10^{-5}, (□) 2.15×10^{-6}, (△,◇) 2.10×10^{-6}.

TABLE II Flow stress–strain rate properties of thermomechanically processed γ/γ'–α at 1000° C

Thermomechanical processing		Flow stress (MPa)		
Number of cycles	Swageing temperature (° C)	Approximate strain rates (sec^{-1})		
		2.15×10^{-5}	2.20×10^{-6}	2.15×10^{-7}
As-grown		403	289	231
As-grown [1]		374	277	225
			287	
Annealed 1 h 900° C [1]		382	305	258
				236
Annealed 7 h 900° C		403	295	236
Annealed 13 h 900° C		401	310	240
			297	
Annealed 22 h 900° C		404	305	234
2	900	420	320	235
4	900	444	325	218
				219
7	900	444	333	200
				204
3	25	444	330	263
				268
5	25	440	326	226
7	25	447	332	222

initiated for as-grown and thermomechanically processed materials. Several compressive creep curves are shown in Fig. 4. These clearly illustrate that the long-term creep resistance of the swaged material is better than that of the as-grown alloy. The apparent large degree of transient creep strain ($\sim 1\%$) for RT13 is unusual, and its source is unknown. Possibly this strain is due to some rapid rearrangement of the dislocation structure imparted by strain–annealing.

Steady-state creep rates and flow stresses taken from the constant-load tests as well as those determined from constant velocity testing are presented in Fig. 5 for as-grown and RT13 materials. All data were fitted to the standard empirical power law model.

$$\dot{\varepsilon} = A\sigma^n \qquad (1)$$

by linear regression techniques, where A is a constant and n is the stress exponent. Values of the coefficient of Determination, R^2, and appropriate equations from this analysis are shown in Fig. 5. While most constant-load tests were designed to produce low strain rates, one RT13 specimen was tested at a high stress to $\sim 10\%$ strain (insert in Fig. 4b), and its behaviour is in good agreement with the constant-velocity results. Use of dummy variables in conjunction with Equation 1 for both material conditions demonstrated that there is no statistical difference (95% level) between the two test methods.

3.3. Post-test microstructure

Both crept as-grown and RT13 specimens were examined by TEM to determine if microstructural features indicative of a changing creep mechanism could be found. Examples of this effort are illustrated in Fig. 6. Some characteristics were common to both conditions: the misfit dislocations between γ and γ' are visible and the fibres contain a few precipitates, are essentially dislocation-free and have rounded corners. The major differences were (i) the as-grown sample possessed thick dislocation walls in γ' at the matrix–fibre interface while similar walls were very thin or non-existent in RT13, and (ii) dislocation networks were formed in the γ' matrix of RT13 but were absent in the as-grown alloy. This seems to indicate that the active creep mechanism has been changed from fibres impeding the dislocation motion (Fig. 6a) to dislocations being held up by networks in the matrix (Fig. 6b).

4. Discussion

The current results for γ/γ'–α indicate that the 1000° C creep strength can be improved by strain–anneal cycles involving room-temperature work and 900° C heat treatments. Such TMP yields a loose three-dimensional dislocation network which rearranges itself into a subgrain boundary structure during creep with γ and α fibres serving as pinning points (Fig. 6b). This behaviour is consistant with the concepts of Sherby, Klundt, and Miller [7] who called attention to the role of subgrain size on creep properties and suggested how such a dislocation structure could be introduced into and maintained in multiphase materials. Since one example of a sub-boundary structure in an as-grown γ/γ'–α alloy (Ni–26.4 Mo–8.3 Al) after stress rupture testing at 825° C has been found [8], it is possible that the dislocation structure of RT13 simply extends the useful range of a normally lower-temperature strengthening mechanism rather than establishing an entirely new deformation mode.

From the flow stress–strain rate data (Table II), it seems that all strain–anneal schedules can improve the 1000° C creep strength at fast rates, but at $\dot{\varepsilon} \lesssim 2 \times 10^{-7} sec^{-1}$ only RT13 processing is effective. Possibly during rapid straining any type of residual structure can impede the dislocations, causing plastic flow and yield equivalent strengths. However under slow deformation rates most residual structures act as dislocation sources rather than barriers. At present the difference in behaviour between strain–anneal cycles involving small amounts of 900° C or room-temperature work is not understood. The TEM microstructures for these TMPs (Figs. 2c and d) are similar,

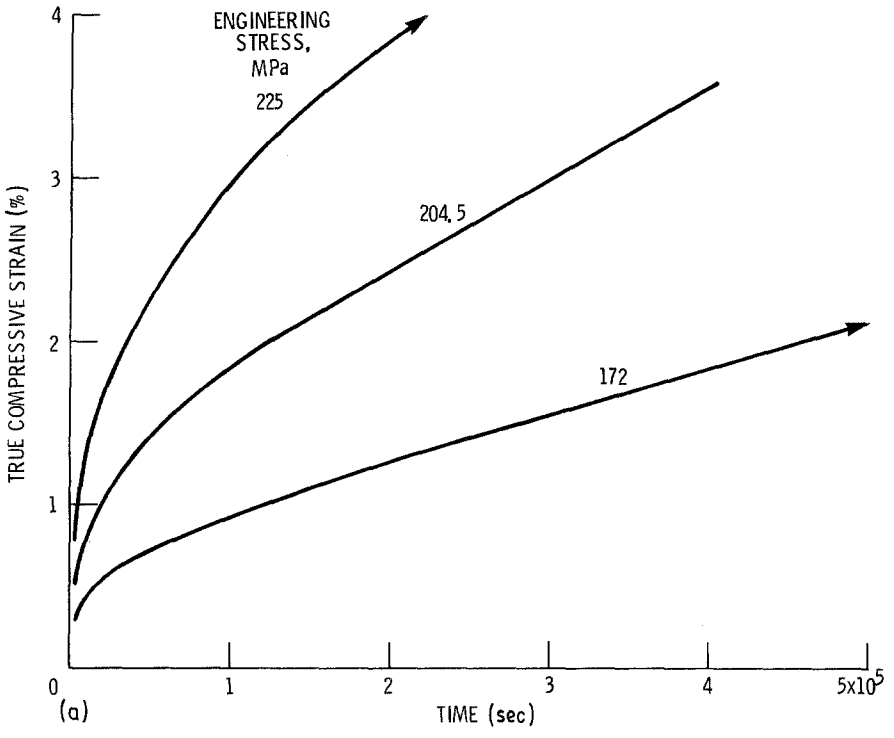

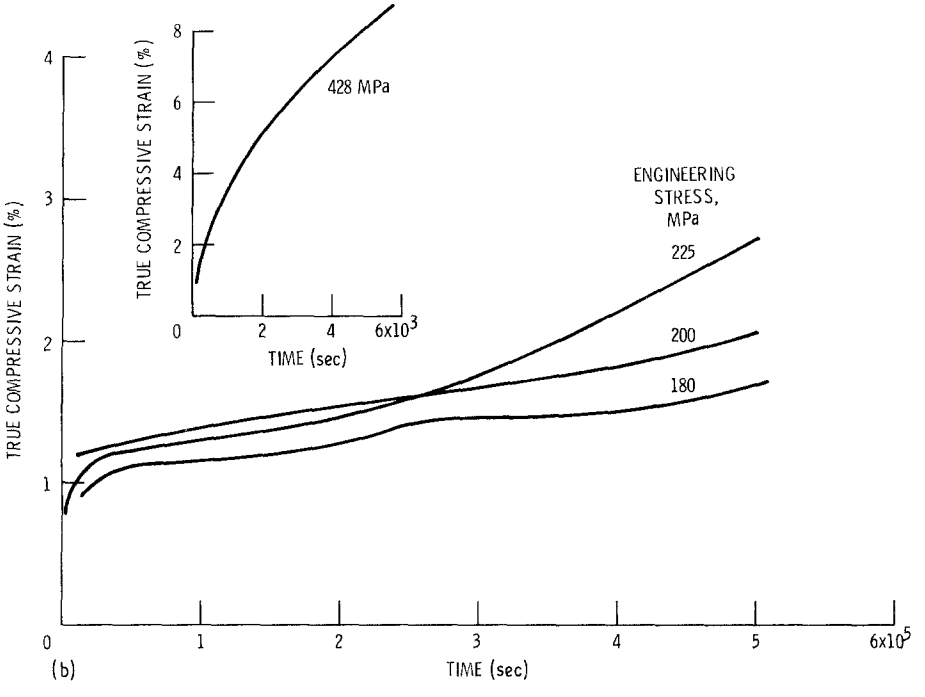

Figure 4 Constant-load compressive creep curves for $\gamma/\gamma'-\alpha$ as a function of engineering stress. (a) As-grown, (b) three strain–anneal cycles with room-temperature swageing.

yet the strength of the 900° C swaged materials is no better than that of as-grown or annealed $\gamma/\gamma'-\alpha$.

In addition to the sub-boundary structure, the improved creep strength of the RT13 condition could be, at least partially, due to several other sources: 900° C annealing and/or reduction in interfibre spacing. If the latter were the controlling process, then strength should increase with the level of work. This is not the case, as creep strength either remains constant or decreases with higher amounts of strain (Table II and [1]) in almost all instances. While decreasing fibre spacing by working does not directly improve properties, statistical examination of the creep behaviour of as-grown and annealed $\gamma/\gamma'-\alpha$ indicated that heat treatment alone somewhat affects strength; however the improvement is slight (Fig. 5) in comparison to the RT13 processing. Attempts to correlate this improvement with time at 900° C were unsuccessful; apparently any prior exposure will increase the 1000° C creep resistance a small amount. Other than the precipitation in the molybdenum-rich fibres (Fig. 2b), there is little evidence as to the source for this additional strengthening. Molybdenum precipitation in γ', similar to that observed by Ishii, Dequette and Stoloff [9] after 850° C annealing of a Ni–31.2 Mo–6.3 Al material, was not found after 900° C heat treatments (Fig. 2b): hence second phases in γ' do not appear to be the reason for increased strength after annealing.

Statistical modelling of the flow stress–strain rate behaviour for as-grown, annealed and RT13 conditions was undertaken to determine whether the differences in properties could be ascribed to the power-

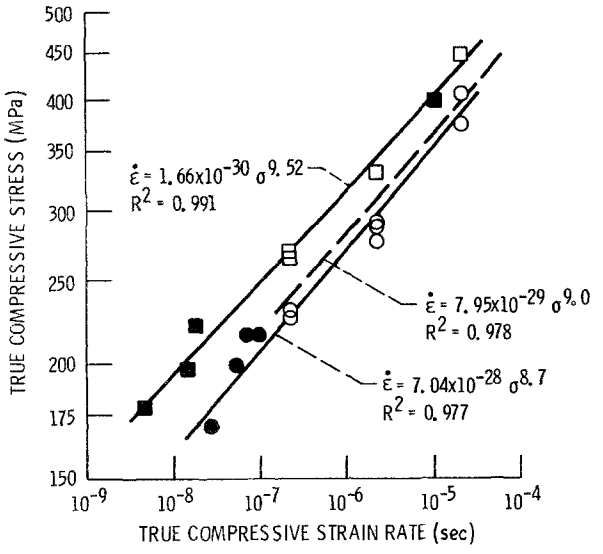

Figure 5 True compressive flow-stress–strain rate behaviour for (○) as-grown $\gamma/\gamma'-\alpha$, and (□) material subjected to three strain–anneal cycles with 13% room-temperature work (RT13). Filled symbols designate constant-load creep tests. Dashed line indicates the behaviour of materials annealed at 900° C.

law constant or stress exponent. While the use of dummy variables clearly indicated that RT13 is different from either the as-grown or annealed $\gamma/\gamma'-\alpha$, it was not possible to assign the strength advantage of RT13 solely to a change in A or n. This results because the standard deviations for the stress exponent and constant are about 0.4 and a factor of 10, respectively, for each curve in Fig. 5 while the values for n and A are similar.

The results of this study indicate that the 1000° C creep properties of $\gamma/\gamma'-\alpha$ can be improved by multiple strain–anneal cycles with small amounts of work at room temperature and annealing at 900° C. Since there is no reason to suspect that 13% strain is optimum, future efforts should investigate overall strain levels ranging from 5 to 20%. However, as the slight improvement in creep properties with annealing was not dependent on time, studies varying the length of the 900° C anneals following swageing do not seem warranted. The effect of non-uniform working techniques should also be examined, and finally the influence of an RT13 schedule on lower-temperature mechanical properties must be determined.

5. Summary of results

The influence of multiple strain–anneal cycles involving swageing at 900° C or room temperature followed by 900° C annealing on the 1000° C creep strength of $\gamma/\gamma'-\alpha$ has been examined. This effort revealed that

1. All TMP schedules improved the creep strength at strain rates $\gtrsim 2 \times 10^{-6}\,\text{sec}^{-1}$.
2. At low strain rates only the RT13 condition which consisted of three room-temperature cycles to 13% strain resulted in a strength improvement.
3. Transmission electron microscopy revealed that creep-tested RT13 material possessed subgrains in the matrix, while they were absent in deformed as-grown $\gamma/\gamma'-\alpha$.
4. Creep behaviour under constant-load conditions is identical to that under constant-velocity conditions.

References

1. J. D. WHITTENBERGER and G. WIRTH, *J. Mater. Sci.* **18** (1983) 2581.
2. M. F. HENRY, M. R. JACKSON and J. L. WALTER, NASA Report CR-135151 (1978).
3. M. F. HENRY, M. R. JACKSON, M. F. X. GIGLIOTTI and P. B. NELSON, NASA Report CR-159416 (1979).
4. J. D. WHITTENBERGER, *Met. Trans. A.* **10A** (1979) 1285.

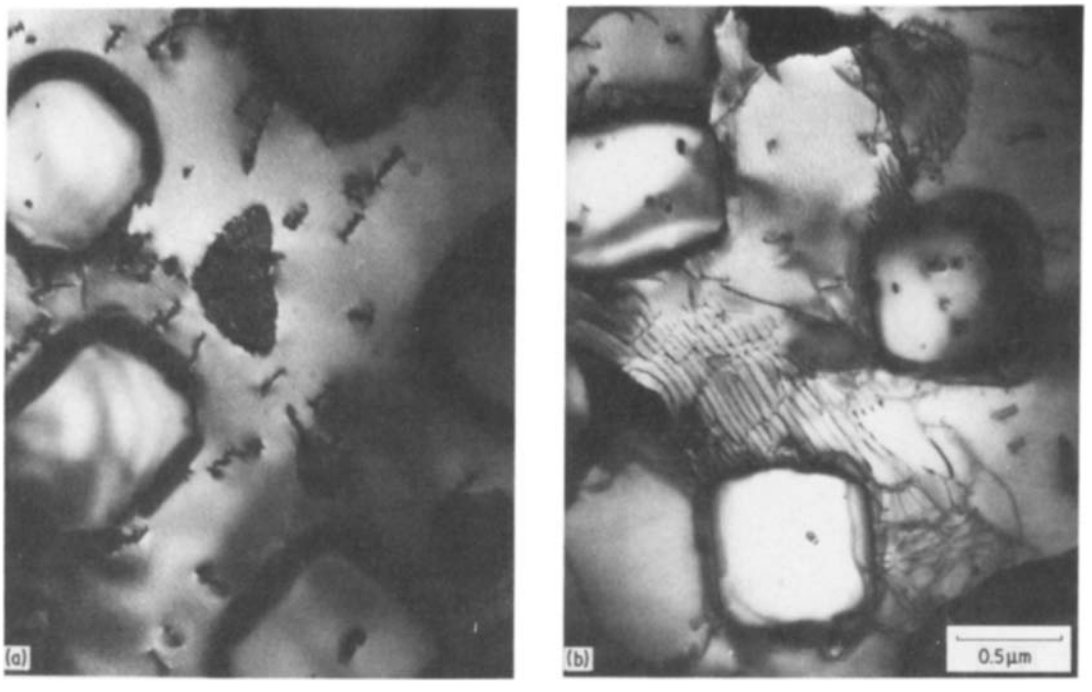

Figure 6 Typical TEM microstructures of $\gamma/\gamma'-\alpha$ creep-tested at 1000° C in air under constant-load conditions. (a) As-grown tested for 6.66×10^5 sec to −2.5% strain under an engineering stress of 172 MPa, (b) RT13 tested for 5.83×10^5 sec to −2.3% strain under an engineering stress of 200 MPa.

5. J. D. WHITTENBERGER and G. WIRTH, *Met. Sci.* **16** (1982) 383.
6. J. D. WHITTENBERGER, *Mater. Sci. Eng.* **57** (1983) 77.
7. O. D. SHERBY, R. H. KLUNDT and A. K. MILLER, *Met. Trans A* **8A** (1977) 843.
8. J. M. TARTAGLIA and N. S. STOLOFF, *ibid.* **12A** (1981) 1891.
9. T. ISHII, D. J. DUQUETTE and N. S. STOLOFF, *Acta Metall.* **29** (1981) 1467.

Received 11 April
and accepted 21 May 1985